

Supporting Information

A DNA Sensor Based on Upconversion Nanoparticles and 2D Dichalcogenide Materials

Konstantina Alexaki,^{a, ‡} Davide Giust,^{a, ‡} Maria-Eleni Kyriazi,^a Afaf H. El-Sagheer,^{b,c} Tom Brown,^b Otto L. Muskens,^{a,d} and Antonios G. Kanaras^{a,d}*

^a School of Physics and Astronomy, Faculty of Engineering and Physical Sciences, University of Southampton, Southampton SO17 1BJ, UK.

^b Department of Chemistry, University of Oxford, Chemistry Research Laboratory, 12 Mansfield Road, Oxford OX1 3TA, UK.

^c Chemistry Branch, Department of Science and Mathematics, Faculty of Petroleum and Mining Engineering, Suez University, Suez 43721, Egypt.

^d Institute for Life Sciences, University of Southampton, Southampton SO17 1BJ, UK.

[‡] These authors contributed equally.

* Corresponding author: a.kanaras@soton.ac.uk

Table of Contents

- S - I Characterization of UCNPs**

- S – II Characterization of PAA and ssDNA / PAA coated UCNPs**

- S - III Characterization of 2D materials**

- S - IV Synthesis of oligonucleotide sequences**

- S - V References**

S - I Characterization of UCNPs

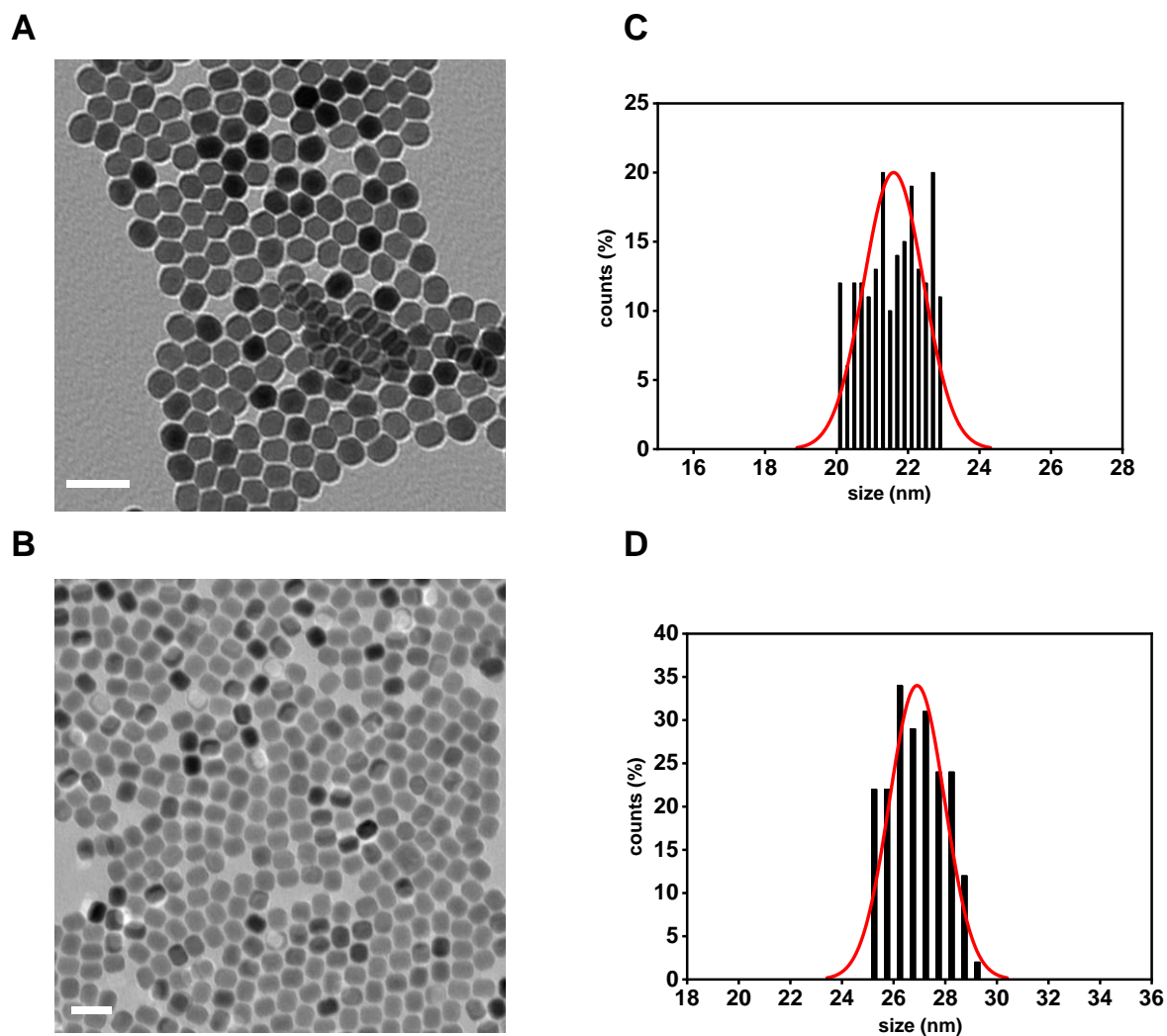


Figure S1. Transmission Electron Images of UCNPs. (A) Core upconversion nanoparticles (NaYF_4 : Yb^{3+} (18%); Er^{3+} (2%) and corresponding size distribution (C). (B) Core-shell upconversion nanoparticles (NaYF_4 : Yb^{3+} (18%); Er^{3+} (2%) @ NaYF_4) and corresponding size distribution (D). Scale bars are 50 nm.

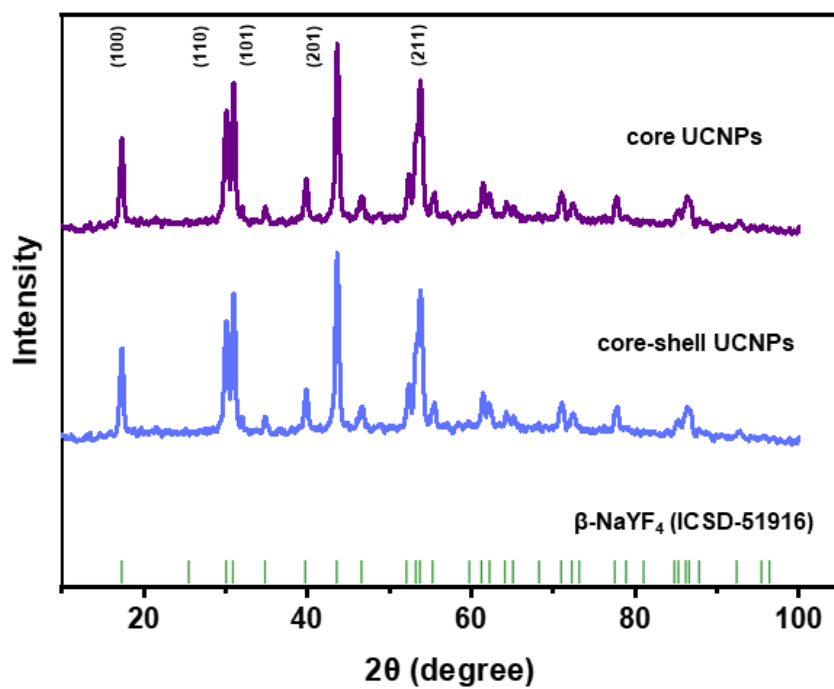


Figure S2. X-ray diffraction spectra of core and core-shell UCNPs confirming the hexagonal crystallinity of the host lattice. The vertical lines on the x axis correspond to the standard pattern for the hexagonal phase NaYF₄: Yb; Er nanoparticles.

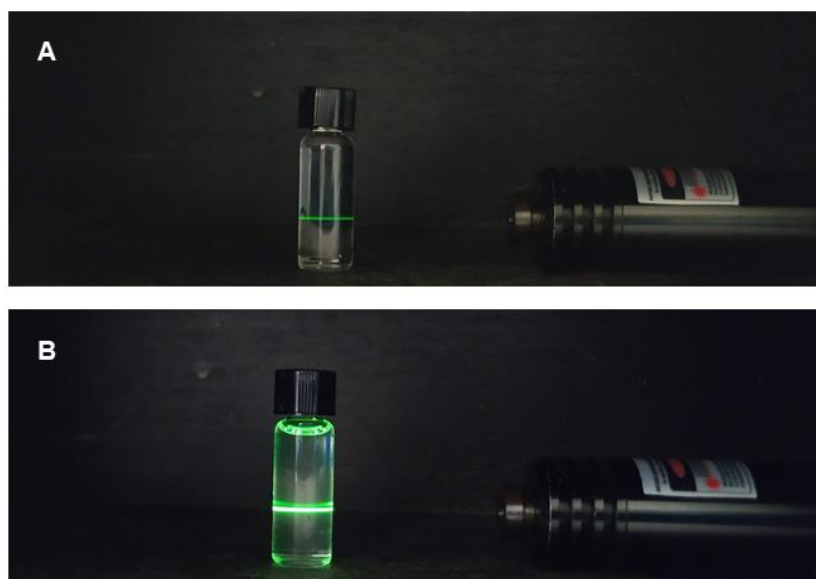


Figure S3. Digital photographs of core UCNPs (A) and core-shell UCNPs (B) in hexane irradiated with a 980 nm laser beam.

S - II Characterization of PAA and ssDNA / PAA coated core-shell UCNPs

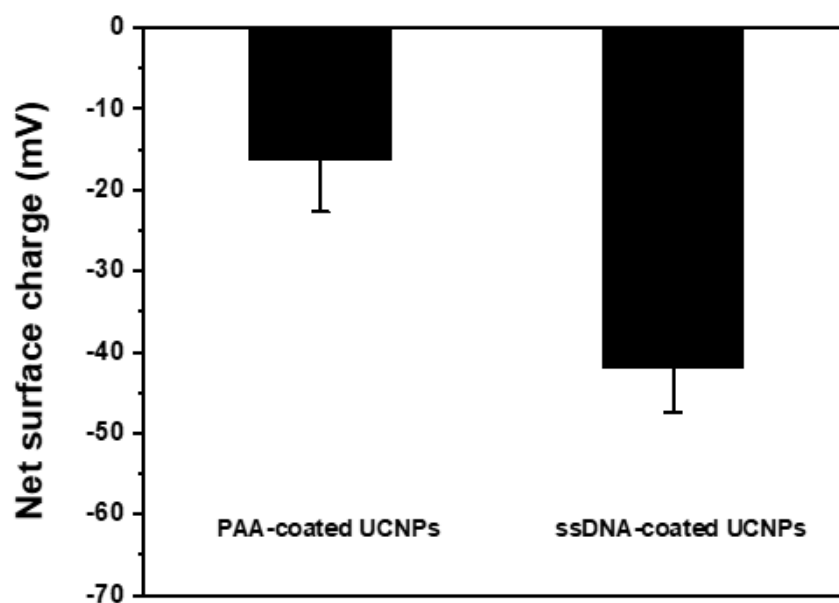


Figure S4. Zeta potential measurements of PAA coated core-shell UCNPs and single-stranded DNA / PAA coated core-shell UCNPs ($0.5 \text{ mg}\cdot\text{mL}^{-1}$).

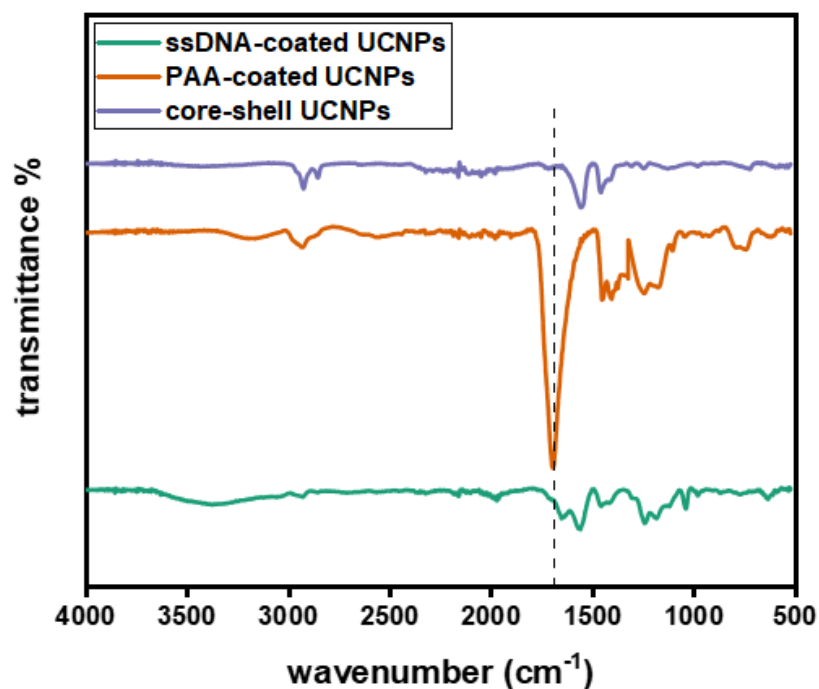


Figure S5. Fourier-transform infrared spectroscopic measurements of oleate-capped core-shell UCNPs, PAA coated core-shell UCNPs and single-stranded DNA / PAA coated core-shell UCNPs. The presence of PAA is confirmed by the appearance of a strong COOH peak at 1700 cm⁻¹. The appearance of the peaks at 1650 cm⁻¹ and 1560 cm⁻¹ is related to the creation of amide bonds due to the conjugation of the oligonucleotides *via* EDC coupling.

S - III Characterization of 2D materials

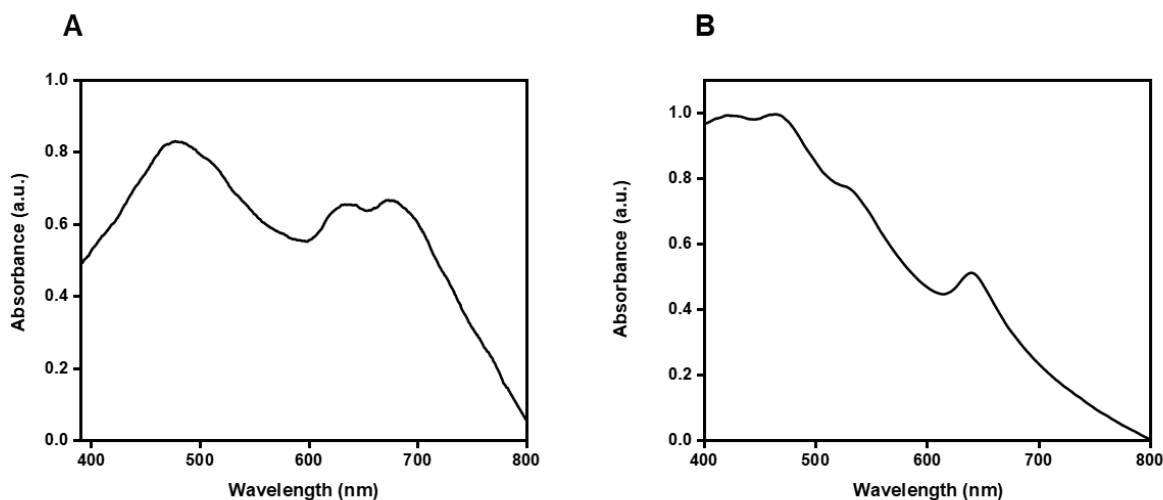


Figure S6. Ultraviolet–visible spectroscopy spectra for MoS₂ (A) and WS₂ (B) dispersed in phosphate buffer saline (0.5 mg·mL⁻¹). MoS₂ is dark green whereas WS₂ appears brown when dispersed in phosphate buffer saline. The absorption features of these two materials correspond well with the typical spectra in the literature.[1-3]

S - IV Synthesis of oligonucleotide sequences

5'-Amino and unmodified oligonucleotides were synthesized on an Applied Biosystems 394 automated DNA/RNA synthesizer using a standard 1.0 μ mole phosphoramidite cycle of acid-catalyzed detritylation, coupling, capping, and iodine oxidation. Stepwise coupling efficiencies and overall yields were determined by the automated trityl cation conductivity monitoring facility and was >98.0%. Standard DNA phosphoramidites and 5'-TFA-Amino-Modifier C6-CE Phosphoramidite were purchased from Link Technologies Ltd. Additional reagents were purchased from Link Technologies Ltd, Sigma-Aldrich, Glen research and Applied Biosystems Ltd. All β -cyanoethyl phosphoramidite monomers were dissolved in anhydrous acetonitrile to a concentration of 0.1 M immediately prior to use with coupling time of 50 s for normal A, G, C, and T monomers and was extended to 600 s for the amino modified monomer. Cleavage and

deprotection were achieved by exposure to concentrated aqueous ammonia solution for 60 min at room temperature followed by heating in a sealed tube for 5 h at 55 °C. Purification was carried out by reversed-phase HPLC on a Gilson system using a Brownlee Aquapore column (C8, 8 mm x 250 mm, 300Å pore) with a gradient of acetonitrile in triethylammonium bicarbonate increasing from 0% to 50% buffer B over 30 min with a flow rate of 4 mL/min (buffer A: 0.1 M triethylammonium bicarbonate, pH 7.0, buffer B: 0.1 M triethylammonium bicarbonate, pH 7.0 with 50% acetonitrile). Elution was monitored by ultraviolet absorption at 298 nm. After HPLC purification, oligonucleotides was freeze dried then dissolved in water without the need for desalting. All Purified oligonucleotides were characterised by electrospray mass spectrometry. Mass spectra of oligonucleotides were recorded either using a XEVO G2-QTOF MS instrument in ES- mode. Data were processed using MaxEnt and in all cases confirmed the integrity of the sequences.

Table S1. Oligonucleotide sequences. X: aminohexyl modification

Name	Oligonucleotide sequences (5' to 3') and modifications
polyT	X – TTT TTT TTT TTT TTT TTT TTT
polyA	AAA AAA AAA AAA AAA AAA AAA
Non-complementary	CTA GAT CCG TGT CCT CGT GGC CGC

S - V References

1. Dumcenco D, Ovchinnikov D, Marinov K, Lazic P, Gibertini M, Marzari N, Sanchez O L, Kung Y C, Krasnozhan D, Chen M W, et al. Large-Area Epitaxial Mono layer MoS₂. *Acs Nano*, 2015, 9(4): 4611-4620.
2. Dong N N, Li Y X, Feng Y Y, Zhang S F, Zhang X Y, Chang C X, Fan J T, Zhang L, Wang J. Optical Limiting and Theoretical Modelling of Layered Transition Metal Dichalcogenide Nanosheets. *Scientific Reports*, 2015, 5.
3. Mishra A K, Lakshmi K V, Huang L P. Eco-friendly synthesis of metal dichalcogenides nanosheets and their environmental remediation potential driven by visible light. *Scientific Reports*, 2015, 5.